개선된 진동기초 손상검색방법의 유도와 검증

Improved Vibration-Based Damage Identification Method

김 정 태* 노리스 스텁스**
Kim, Jeong-Tae Stubbs, Norris

요 지

본 논문에서는 새로이 유도된 진동기초 손상검색방법을 제시하고, 제한적인 모드특성치가 측정된 구조물을 대상으로 이 알고리즘의 적합성과 손상예측의 정확도를 검증하고자 하였다. 먼저, 기존의 Kim과 Stubbs[16,17]에 의해 발표된 손상발견 알고리즘들을 검토하였으며, 이 알고리즘들의 적용한계와 오류적 가정을 극복할 수 있는 손상검색 알고리즘을 새로이 유도하였다. 다음으로, 손상발생 전후에 소수의 진동모드 특성치가 측정된 2경간 연속보를 대상으로 손상예측실험을 수행하여 이들 손상검색 알고리즘의 손상예측 정확도를 분석하였다. 기존의 손상검색 알고리즘에 비하여 새로이 유도된 손상검색 알고리즘의 손상예측 정확도가 향상된 것으로 분석되었다.

핵심용어 : 구조식별, 진동기초, 손상검색, 모드실험, 모드해석

Abstract

In this paper, a newly-derived algorithm to predict locations and severities of damage in structures using modal characteristics is presented. Its feasibility and the accuracy of damage prediction are evaluated in structures for which limited modal parameters are available. Two existing damage detection algorithms, proposed by Kim and Stubbs[16,17], are reviewed and the new algorithm is formulated to improve the accuracy of damage localization and severity estimation by eliminating erratic assumptions and limits in the existing algorithms. The damage prediction accuracy is assessed when applied to a two-span continuous beam for which pre-damage and post-damage modal parameters are available for only a few modes of vibration. Compared to the existing damage detection algorithms, the newly-derived algorithm improved the accuracy of damage localization and severity estimation results in the test beam.

Keywords : *system identification, vibration-based, damage detection, modal test, modal analysis*

1. Introduction

This paper deals with the general problem of utilizing changes in dynamic modal parameters of structures to nondestructively detect, locate, and estimate the severity of damage in these structures. Structural damage may be defined as any deviation of a geometric or

* 정회원 · 부경대학교 해양공학과, 조교수
** A.P. and Florence Wiley Professor, Department of Civil Engineering, Texas A&M University, USA

• 이 논문에 대한 토론을 1999년 12월 31일까지 본 학회에 보내주시면 2000년 3월호에 그 결과를 게재하겠습니다.

material property defining a structure that may result in unwanted responses of the structure. A solution to this problem is important for at least two reasons. Firstly, damage localization and severity estimation are the first two steps in the broader category of damage assessment. Secondly, a timely damage assessment could produce desirable consequences such as saving of lives, reduction of human suffering, protection of property, increased reliability, increased productivity of operations, and reduction in maintenance costs.

During the past decade, a significant amount of research has been conducted in the area of damage detection using the dynamic response of a structure. Research efforts have been made to detect structural damage directly from dynamic response measurements in the time domain, e.g., the Random Decrement technique[1),2)], or from Frequency Response Functions (FRF)[3)]. Also, methods have been proposed to detect damage using system identification techniques[4),5)]. Many research studies have been conducted in the area of nondestructive damage detection(NDD) using changes in modal parameters. Research studies have related changes in eigenfrequencies to changes in beam properties such as cracks, notches or other geometrical changes[6)~8)]. Studies have also focused on the possibility of using the vibration characteristics of structures as an indication of structural damage[9)~12)]. Since 1988, studies on the topic appear to be accelerating. Attempts have been made to monitor structural integrity of bridges[3),13)], to investigate feasibility of damage detection in large space structures using changes in modal parameters[14),15)], and to localize damage in beamtype structures using changes in mode shapes characteristics[16)~18)].

Despite these research efforts, however, many problems related to vibration-based damage detection remain unsolved today. Outstanding needs remain to locate and estimate the severity of damage: (a) in structures with only few available modes, (b) in structures with many members, (c) in structures for which baseline modal responses are not available, and (d) in an environment of uncertainty associated with modeling, measurement, and processing errors.

In this paper, we present an improved vibration-based NDD algorithm to locate and estimate severity of damage in structures. The proposed methodology is presented here in two parts. In the first part, we outline vibration-based NDD algorithms. We first review existing NDD algorithms proposed by Kim and Stubbs[16),17)]. Then we formulate a new NDD algorithm to improve its accuracy in damage localization and severity estimation by eliminating erratic assumptions and limits in the existing NDD algorithms. In the second part, we demonstrate the feasibility of the newly-derived NDD algorithm using numerical examples. The new NDD algorithm and two existing ones are evaluated by predicting damage locations and estimating severities of damage in a two-span continuous beam for which limited modal parameters are available for a few modes of vibration. The performance of each NDD algorithm is assessed by quantifying the accuracy of damage localization and severity estimation results.

2. Existing Damage Detection Algorithm (by Kim and Stubbs[16),17)])

For a linear, undamaged, skeletal structure with *ne* elements and *n* nodes, the *i*th modal stiffness of the arbitrary structure is given by

$$K_i = \Phi_i^T C \Phi_i \tag{1}$$

where Φ_i is the ith modal vector and C is the system stiffness matrix. The contribution of jth member to ith modal stiffness, K_{ij}, is given by

$$K_{ij} = \Phi_i^T C_j \Phi_i \tag{2}$$

where C_j is the contribution of jth member to the system stiffness matrix. Then, the fraction of modal energy(i.e., the undamaged modal sensitivity) of the ith mode and the jth member is defined as

$$F_{ij} = K_{ij}/K_i \tag{3}$$

Let the corresponding modal parameters in Eqs. 1 to 3 associated with a subsequently damaged structure be characterized by asterisks. Then for the damaged structure, the damaged sensitivity of the ith mode and the jth member is defined as

$$F_{ij}^* = K_{ij}^*/K_i^* \tag{4}$$

in which the quantities K_{ij}^* and K_i^* are given by

$$K_{ij}^* = \Phi_i^{*T} C_j^* \Phi_i^*, \quad K_i^* = \Phi_i^{*T} C^* \Phi_i^* \tag{5a,b}$$

The quantitie C_j and C_j^* in Eq. 2 and Eq. 5(a) may be written as follows;

$$C_j = E_j C_{jo}; \quad C_j^* = E_j^* C_{jo} \tag{6a,b}$$

where the scalars E_j and E_j^* are parameters representing material stiffness properties of undamaged and damaged jth members, respectively. The matrix C_{jo} involves only geometric quantities(and possibly terms containing Poisson's ratio) and it can represent beam or plate elements.

2.1 First Approximation of NDD Algorithm - Damage Index A[16]

Suppose we make an approximation that the modal sensitivities for the ith mode and the jth location is the same for both undamaged and damaged structure(i.e., $F_{ij}^* \approx F_{ij}$). Then Eqs. 3 and 4 are combined and reduced to the following expression:

$$F_{ij}^*/F_{ij} = (K_{ij}^* K_i)/(K_{ij} K_i^*) = 1 \tag{7}$$

On substituting Eqs. 1, 2, 5, and 6 into Eq. 7 and rearranging, a damage index β_j of jth member(and for nm vibrational modes involved) is obtained by[16]

$$\beta_j = \frac{E_j}{E_j^*} = \frac{\sum_{i=1}^{nm} \gamma_{ij}^* K_i}{\sum_{i=1}^{nm} \gamma_{ij} K_i^*} \tag{8}$$

in which $\gamma_{ij} = \Phi_i^T C_{jo} \Phi_i$ and $\gamma_{ij}^* = \Phi_i^{*T} C_{jo} \Phi_i^*$ and damage is indicated at jth member if $\beta_j > 1$.

The severity of damage in the jth member is estimated as follows. Let the fractional change in the stiffness of the jth member be given by the severity estimator, α_j, then

$$E_j^* = E_j\left(1 + \frac{dE_j}{E_j}\right) = E_j(1+\alpha_j) \tag{9}$$

Combining Eq. 8 and Eq. 9 yields[16]

$$\alpha_j = \frac{\sum_{i=1}^{nm} \gamma_{ij} K_i^*}{\sum_{i=1}^{nm} \gamma_{ij}^* K_i} - 1, \alpha_j \geq -1 \tag{10}$$

where damage severity is indicated as the reduction in stiffness in the jth member if $\alpha_j < 0$.

2.2 Second Approximation of NDD Algorithm - Damage Index B[17)]

From Eq. 8, damage is indicated at jth member if $\beta_j > 1$. However, Eq. 8 becomes singular if the denominator goes zero. This will occur when simultaneously, the element size approaches zero and the element location coincides with a nodal point of a vibrational mode. To overcome this limitation(i.e., the division by zero difficulty), an approximation is made such that the axis of reference for the modal sensitivities is shifted by a value of 1.0(i.e., $F_{ij} \rightarrow F_{ij}+1$ and $F^*_{ij} \rightarrow F^*_{ij}+1$). Add- ing unity to both the numerator and the denominator of Eq. 7 yields

$$(F^*_{ij}+1)/(F_{ij}+1)=[(K^*_{ij}+K^*_i)K_i]/[(K_{ij}+K_i)K^*_i]=1 \tag{11}$$

On substituting Eqs. 1, 2, 5, and 6 into Eq. 11 and rearranging, a damage index β_j of jth member(and for nm modes) is obtained by [17)]

$$\alpha_j=\frac{E_j}{E^*_j}=\frac{\sum_{i=1}^{nm}\left(\gamma^*_{ij}+\sum_{k=1}^{ne}\gamma^*_{ik}\right)K_i}{\sum_{i=1}^{nm}\left(\gamma_{ij}+\sum_{k=1}^{ne}\gamma_{ik}\right)K^*_i} \tag{12}$$

where damage is indicated at the jth location if $\beta_j > 1$.

Once damage is located at the jth member, damage severity is estimated by combining Eq. 12 and Eq. 9 [16)].

$$\alpha_j=\frac{\sum_{i=1}^{nm}\left(\gamma_{ij}+\sum_{k=1}^{ne}\gamma_{ik}\right)K^*_i}{\sum_{i=1}^{nm}\left(\gamma^*_{ij}+\sum_{k=1}^{ne}\gamma^*_{ik}\right)K_i}-1,\quad \alpha_j \geq -1 \tag{13}$$

where damage severity is indicated as the reduction in stiffness in the jth member if $\alpha_j < 0$.

3. Newly-Derived Damage Detection Algorithm - Damage Index C

Let λ_i and λ^*_i are the ith eigenvalues of pre-damage and post-damage $mdof$ structural systems, respectively. Then the ith eigenvalues can be related to the following forms:

$$\lambda^*_i=\lambda_i+d\lambda_i=(K_i+dK_i)/(M_i+dM_i) \tag{14}$$

in which K_i and M_i are the ith modal stiffness and the ith modal mass of the undamaged system, respectively. Also, $d\lambda_i$, dK_i, dM, are the change in the ith eigenvalues, the change in the ith modal stiffness, and the change in the ith modal mass in the system.

On expanding and rearranging Eq. 14, we obtain

$$\frac{dK_i}{K_i}=\frac{d\lambda_i}{\lambda_i}+\frac{dM_i}{M_i}\left(1+\frac{d\lambda_i}{\lambda_i}\right) \tag{15}$$

where dK_i/K_i represents the fractional change of the ith modal stiffness and all the terms in the right hand side of the above equation can be determined directly or via experimental measurements.

For the ith mode and the jth location, the undamaged and damaged modal sensi- tivities, F_{ij} and F^*_{ij} are related by the equation

$$F^*_{ij}=F_{ij}+dF_{ij} \tag{16}$$

where dF_{ij} represents the change fractional of modal energy at the jth member and for

the ith mode. On differentiating Eqs. 3 and 16, the quantity dF_{ij} can be obtained from the expression:

$$dF_{ij}=\frac{K_{ij}}{K_i}\left[\frac{dK_{ij}}{K_{ij}}-\frac{dK_i}{K_i}\right] \tag{17}$$

where dK_{ij} represents the fractional change in K_{ij}. Also, by noticing $K_i \gg K_{ij}$, Eq. 17 can be reduced to the following form:

$$dF_{ij}\cong\frac{dK_{ij}}{K_i} \tag{18}$$

Next, combining Eq. 2 and Eq. 6 and also Eq. 5 and Eq. 6, respectively, gives

$$K_{ij}=\gamma_{ij}E_j,\quad K^*_{ij}=K_{ij}+dK_{ij}=\gamma^*_{ij}E^*_j \tag{19a,b}$$

in which $\gamma_{ij}=\Phi^*_i C_{jo}\Phi_i$ and $\gamma^*_{ij}=\Phi^{*T}_i C_{jo}\Phi^*_i$. Also from Eq. 19, dK_{ij} can be rewritten by

$$dK_{ij}=\gamma^*_{ij}(E_j+dE_j)-\gamma_{ij}E_j \tag{20}$$

On dividing both sides of Eq. 20 by K_i (assuming $K_i\approx\gamma_i E_j$), substituting into Eq. 19, and only solving for the fractional change in the jth members stiffness, we obtain

$$\frac{E_j}{E_j+dE_j}=\left(\frac{\gamma^*_{ij}}{\gamma_i}\right)\Big/\left(\frac{dK_{ij}}{K_i}+\frac{\gamma_{ij}}{\gamma_i}\right) \tag{21}$$

Assuming the structure is damaged at a single location and the resulting change in K_{ij} is only the function of E_j, a first approximation of dK_{ij} can be obtained from the expression:

$$\frac{dK_{ij}}{K_i}=\left(\frac{\partial K_{ij}}{\partial E_j}+\frac{\partial K_{ij}}{\partial\gamma_{ij}}\frac{\partial\gamma_{ij}}{\partial E_j}\right)\frac{dE_j}{K_i} \tag{22}$$

in which

$$\partial K_{ij}/\partial E_j=\gamma_{ij},\quad \partial K_{ij}/\partial\gamma_{ij}=E_j \tag{23a,b}$$

On substituting Eq. 23 into Eq. 22 and further approximation gives

$$\frac{dK_{ij}}{K_i}\cong\frac{\gamma_{ij}}{\gamma_i}\frac{dE_j}{E_j}+\frac{d\gamma_{ij}}{\gamma_i} \tag{24}$$

and

$$d\gamma_{ij}=\gamma^*_{ij}-\gamma_{ij},\quad \gamma_i=\sum_{k=1}^{ne}\Phi_i^T C_{ko}\Phi_i \tag{25}$$

Since we have assumed that the structure is damaged in a single location, it follows readily that $dK_{ij}=dK_i$(note that $dK_{ij}\approx dK_i/nd$ if the structure is damaged in nd multiple locations, in which the nd locations can be predicted). Then by substituting Eq. 15 into Eq. 24, the fractional changes in modal stiffness can be approximately related to the fractional changes in modal properties.

$$\frac{dK_{ij}}{K_i}\cong g_i(\lambda,\Phi)=\left\{\frac{d\lambda_i}{\lambda_i}+\frac{dM_i}{M_i}\left(1+\frac{d\lambda_i}{\lambda_i}\right)\right\}\Big/nd \tag{26}$$

in which $g_i(\lambda,\Phi)$ is the dimensionless factor representing the systematic change in modal parameters of the ith mode due to the damage.

By applying Eqs. 22-26 to Eq. 21, a new damage index for ith mode and jth location is given by

$$\beta_{ji}=\frac{E_j}{E^*_j}=\frac{\gamma^*_{ij}}{\gamma_i g_i(\lambda,\Phi)+\gamma_{ij}}=\frac{Num}{Den} \tag{27}$$

For nm vibrational modes, a damage index β_j for the jth location is obtained by

$$\beta_j=\sum_{i=1}^{nm}Num\Big/\sum_{i=1}^{nm}Den \tag{28}$$

Once damage is located at the jth member, damage severity of the jth member is estimated directly from Eqs. 21, 27 and 28.

$$\alpha_j = dE_j / E_j = 1/\beta_j - 1, \quad \alpha_j \geq -1 \tag{29}$$

where damage severity is indicated as the reduction in stiffness in the jth member if $\alpha_j < 0$.

The method described above yields information on the location and severity of damage directly from changes in mode shapes of structures. The appealing features of this method include the following: (1) damage can be located and sized using a few modes; (2) damage can be located and sized without solving a system of equations; and (3) damage can be located and sized in structures containing many members.

4. Numerical Verification of the Theory

The objective here is to evaluate the feasibility of the proposed algorithm to localize and estimate the severity of damage in a numerical model of a structure when only data on a few modes of vibration are available. We meet this objective in four steps: firstly, a test structure is defined and modal responses of the test structure are generated using the software package ABAQUS; secondly, a damage detection model of the test structure is selected; thirdly, the existing NDD algorithms(Damage Index A and Damage Index B) and the proposed algorithm(Damage Index C) are used to locate and estimate the severity of simulated damage in the test structure; and finally, the accuracy of NDD algorithm are evaluated by quantifying the damage prediction results. Here, by damage detection model we mean a mathematical representation of a structure with degrees of freedom corresponding to actual sensor readings or interpolated readings based on sensor readings at nearby locations.

4.1 Description of Test Structure

The test structure selected here is a theoretical model of a two-span continuous beam.[16),17)] In their previous work, Kim and Stubbs(Ref. 16) identified a realistic theoretical model of a model plate-girder structure by fine-tuning experimental responses and a finite element model of the structure. As shown in Fig. 1, the main structural subsystems of the theoretical model consisted of three element groups: (1) 50 beam members modeling the two-span continuous beam section; (2) two linear axial springs (Spring 1) modeling two outside supports; and (3) a linear axial spring(Spring 2) modeling a middle support. A typical arrangement of the test beam corresponding to 51 nodal points is schematized in Fig. 1. In this hypothetical example we assume that only vertical motion is measured at each nodal point. Values for the material properties of the beam elements and springs were assigned as follows: (1) the elastic modulus; $E = 70Gpa$; (2) Poisson's ratio $v = 0.33$; and (3) the linear mass density $\rho = 2710kg/m^3$. Values for the geometric properties were assigned as follows: (1) for beam elements, the cross-sectional area $A = 1.05 \times 10^{-3} m^2$ and the second moment of area $I = 7.23 \times 10^{-7} m^4$; (2) for Spring 1 member, $A = 4.96 \times 10^{-6} m^2$ and $I \approx 0$; and (3) for Spring 2 member, $A = 8.4 \times 10^{-6} m^2$ and. $I \approx 0$.

Next, we measured, via numerical simulation, the pre-damage and post-damage modal responses of the test structure. Here ten damage cases are investigated, as summarized in Table 1. Each scenario represents a potential

damage event that is typical to the existing beam-type bridges. It is also considered to account for the relationship between the modal sensitivity and the selected damage locations. A few locations which are relatively less sensitive to at least one mode are involved in the damage scenarios.

For example, Case 5 was selected to simulate an element near the middle support. Meanwhile, Case 7 was selected to simulate another element in the middle of the span. The first eight damage cases are limited to the model damaged only at a single location. Cases 6-8 focus on Element 39 in which three magnitude levels of damage are simulated. The last two damage cases (Cases 9 and 10) consider the model damaged in two locations. In all cases, damage was simulated in the structure by reducing the elastic modulus of the appropriate elements. Typical responses which were numerically generated(e.g., mode shapes and frequencies of the first three modes) are shown in Fig. 2 and Table 1.

4.2 Damage Localization and Severity Estimation

We predict locations and severities of damage in the test structure using both the existing NDD algorithms(i.e., Damage Index A and Damage Index B) and the proposed NDD algorithm(i.e., Damage Index C). For each NDD

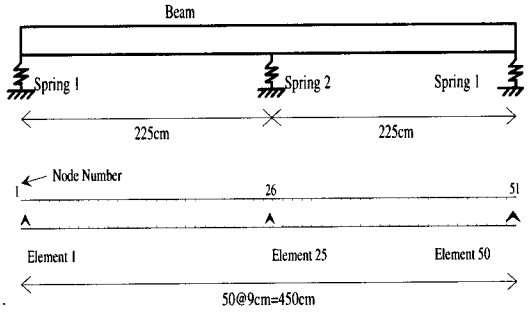

Fig. 1 Schematic of two-span continuous beam

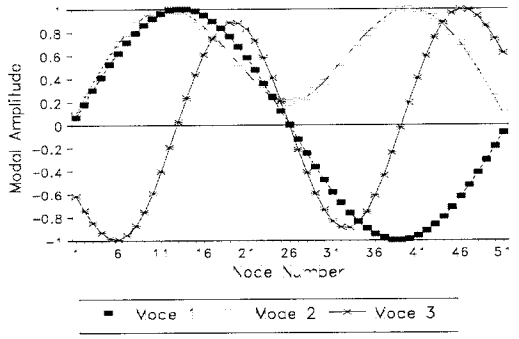

Fig. 2 Mode shapes of two-span continuous beam

Table 1 Damage scenarios and natural frequencies of two-span continuous beam(*Severity (%) = $(E^* - E)/E \times 100$)

Damage Case	Simulated Damage		Natural Frequency(Hz)		
	Location	Severity*	Mode1	Mode2	Mode3
Undamaged	-	-	32.381	46.377	118.77
1	4	-10	32.368	46.356	118.66
2	9	-10	32.328	46.309	118.69
3	14	-10	32.314	46.331	118.74
4	19	-10	32.346	46.376	118.58
5	24	-10	32.379	46.282	118.75
6	39	-10	32.361	46.358	118.77
7	39	-1	32.179	46.188	118.77
8	39	-50	31.371	45.432	118.77
9	9,34	-10, -10	32.276	46.297	118.52
10	14,39	-10, -10	32.247	46.266	118.74

algorithm involved, we perform the damage localization and severity estimation in four steps. In Step One, pre-damage and post-damage modal parameters of the first three modes(as shown and listed in Fig. 2 and Table 1) were obtained from modal analysis of the test structure.

In Step Two, we selected the Euler Bernoulli beam as the damage detection model on the basis of the fact that the test model is a one-dimensional beam with only vertical motions are available. From the mode shape of ith modal vector $\phi_i(x)$, we generated a third order spline function, $w(x)$, for the beam using the 51 nodal displacements. Using the spline approximation of the mode shape, we computed the instantaneous curvature of the mode shape, $\phi_i''(x) = w''(x)$ at the 51 nodes of the test model. Then equivalent expressions for γ_{ij}, γ_{ij}^*, and γ_i in the damage index equations (e.g., Eqs. 8, 12, and 27) are computed by

$$\gamma_{ij} = \int_{x_k}^{x_k+\Delta x_k} \{\phi_i''(x)\}^2 dx,\quad \gamma_{ij}^* = \int_{x_k}^{x_k+\Delta x_k} \{\phi_i''^*(x)\}^2 dx,$$
$$\gamma_i = \int_0^L \{\phi_i''(x)\}^2 dx \qquad (30)$$

in which x_k and $x_k+\Delta x_k$ correspond to two nodal locations of an element j for the beam model.

In Step Three, we established more robust statistical criteria for damage localization. For a given set of modes, the locations of damage are selected on the basis of a rejection of hypotheses in the statistical sense.[19),20)] First, the value β_j $(j=1,2,3,\cdots,ne)$ associated with each member is treated as a random variable β. In other words, the collection of the damage indices β_j represent a sample population(we further assume the variables distributed normally). The normalized indicator is given by

$$Z_j = (\beta_j - \overline{\beta_i})/\sigma_i \qquad (31)$$

in which $\overline{\beta_i}$ and σ_i are mean and standard deviation of the collection of indicators of β_j values, respectively. Next, the member is assigned to damage class via a statistical-pattern-recognition technique that utilizes hypothesis testing. The null hypothesis(i.e., H_0) is that the structure is not damaged at the jth location. The alternate hypothesis (i.e., H_1) is that the structure is damaged at the jth location. We define the decision rule as follows: (1) select H_0(i.e., no damage exists at member j) if $Z_j < 2$ and (2) select the alternate H_1 if $Z_j \geq 2$. This criterion corresponds to a one-tailed test at a significance level of 0.023(97.7 percent confidence level).

For Damage Index A, the damage indicator, Eq. 8, and the above criterion were used to select potential damage location (See Column 4 in Table 2). For Damage Index B, we repeated the exercises using Eq. 12 and predicted potential damage locations(See Column 6 in Table 2). Finally, for Damage Index C, we repeated the same procedures using Eq. 28 and predicted potential damage locations(See Column 8 in Table 2). Among 10 damage cases, three cases were illustrated closely: Damage Case 1(Fig. 3), Damage Case 5(Fig. 4), and Damage Case 10(Fig. 5). Each figure show that Damage Index C has better localization-accuracy than Damage Index A, but it has the same accuracy as Damage Index B(See also Table 2).

In Step Four, damage severities were estimated for the predicted damage locations. For Damage Indices A, B, and C, we estimated

damage severities using Eq. 9, Eq. 13, and Eq. 29, respectively. The estimated results of damage severities are listed in Table 2 as follows: Column 5 for Damage Index A, Column 7 for Damage Index B, Column 9 for Damage Index C. Figs. 3-5 show the accuracy of severity prediction for Damage Cases 1, 5, and 10, respectively. Each figure shows that Damage Index C produced best estimated values. Damage Index A overestimated the severities, while Damage Index B underestimated those values.

4.3 Quantification of Damage Prediction Accuracy[16),20),21)]

The accuracy of damage prediction results was quantified by measuring both metrical errors and the common errors used in tests of hypotheses[16),21)]. In this study, the uncer-

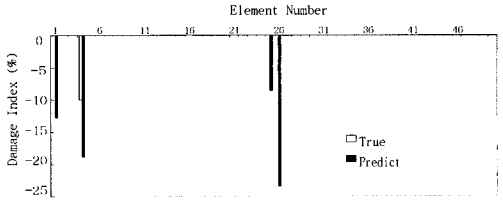

(a) Damage Index A

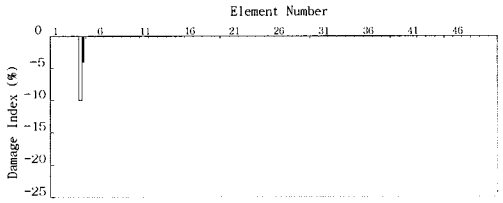

(b) Damage Index B

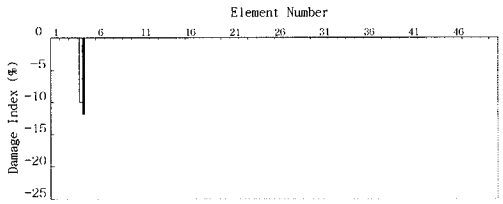

(c) Damage Index C

Fig. 3 Damage prediction results of damage case 1

Table 2 Damage prediction results of two-span continuous beam (*Severity (%) = $(E^* - E)/E \times 100$)

Damage Case	Simulated Damage		Predicted Damage (Damage Index A)		Predicted Damage (Damage Index B)		Predicted Damage (Damage Index C)	
	Location	Severity	Location	Severity	Location	Severity	Location	Severity
1	4	-10	1, 4 25, 26	-12.8, -18,9 -8.6, -23.5	4	-3.8	4	-11.9
2	9	-10	1, 9 26	-11.6, -18.7 -20.9	9	-1.3	9	-10.7
3	14	-10	14, 26	-18.3, -31.4	14	-1.4	14	-9.4
4	19	-10	19, 26	-18.1, -16.8	19	-0.8	19	-9.5
5	24	-10	24, 25 26	-15.7, -18.7 -7.6	24	-0.5	24	-9.3
6	39	-1	25, 26 (-), 49	-11.1, -7.3 (-), -5.2	39	-0.1	39	-1.0
7	39	10	25, 39	-29.0, -18.5	39	-1.5	39	-9.6
8	39	-50	25, 39	-67.2, -72.7	39	-14.8	39	-46.4
9	9,34	0, -10	9, 34 50	-18.3, -17.5, -7.7	9,34	-1.3, -1.1	9,34	-11.1, -8.0
10	14,39	-10, -10	14, 26 39	-17.4, 11.3, -17.7	14,39	-1.4, -1.4	14,39	-10.3, -10.9

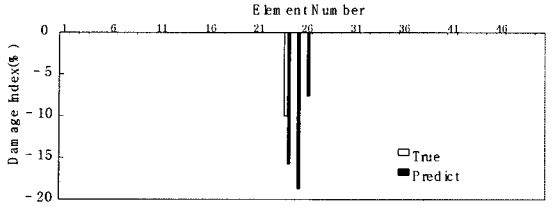

(a) Damage Index A

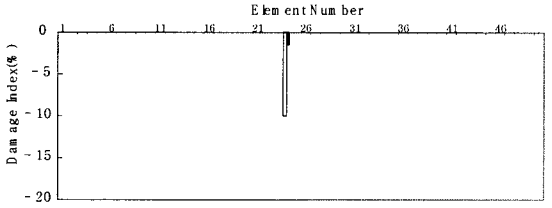

(b) Damage Index B

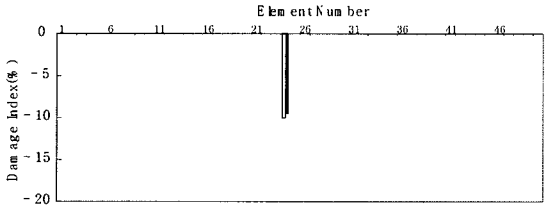

(c) Damage Index C

Fig. 4 Damage prediction results of damage case 5

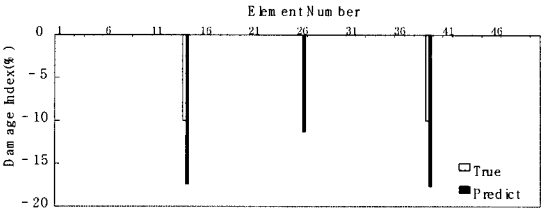

(a) Damage Index A

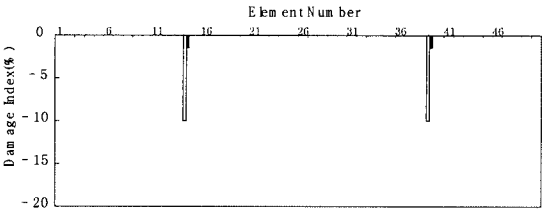

(b) Damage Index B

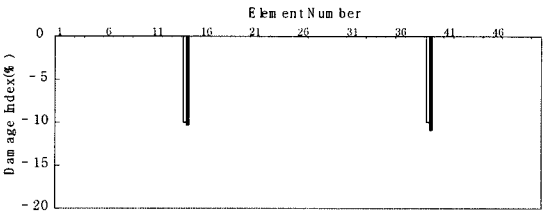

(c) Damage Index C

Fig. 5 Damage prediction results of damage case 10

tainty related to modeling errors, measurement errors, or any other types were not involved in this accuracy assessment. As the first NDD accuracy measure, we selected a mean localization error (*mle*) defined as

$$mle=\frac{1}{N}\sum_{i=1}^{N}\left| x_i^t-x_i^p\right| /L,\ 0\le mle\le 1 \quad (32)$$

where N is the number of damage cases, x_i^t and x_i^p are the true location and the predicted location of the ith damage case, respectively, and L is a characteristic distance(e.g., a span of the beam model).

As the second NDD accuracy measure, we selected a detection missing error(*dme*) defined as

$$dme=\frac{1}{NT}\sum_{i=1}^{N} TI,\ 0\le dme\le 1 \quad (33)$$

where NT is the number of true damage locations, TI is the number of Type I errors (fail-in-detection of true damage locations) for the number of true damage locations. The *dme* measures false negative errors such that true damage locations are not predicted. If $dme = 0$, it means that all true damage locations are predicted.

As the third NDD accuracy measure, we selected a false alarm error (*fae*) defined as

$$fae=\frac{1}{NF}\sum_{i=1}^{N} TII,\ o\le fae<\infty \quad (34)$$

where NF is the number of the predicted

locations, *TII* is the number of Type II errors(prediction of locations that are not damaged). The *fae* measures false-positive errors such that predicted locations are not the true damage locations. If *fae* = 0, then all predicted locations correctly locate the damage.

As the last NDD accuracy measure, we selected a mean sizing error(*mse*) which is defined as

$$mse = \frac{1}{NF} \sum_{i=1}^{N} \left| (\alpha_i^t - \alpha_i^p)/\alpha_i^p \right|, \quad 0 \le mse \le \infty \quad (35)$$

where α_i^t and α_i^p are, respectively, a true damage severity and a predicted damage severity for ith location. The *mse* measures the NDD algorithm's accuracy in severity estimation and the value close to zero means that the severity estimation error is close to zero.

We implemented the four NDD accuracy measures given by Eqs. 32-35 to the damage localization and severity estimation results of each NDD algorithm. Then the accuracy of each NDD algorithm was quantified as listed in Table 3. From the Table, three major results are observed. Firstly, the accuracy measures for Damage Index A are analyzed as follows: (1) a *dme* of 0.083 indicates that eleven out of twelve true damage locations can be predicted; (2) a *fae* of 0.57 indicates that about six out of ten predicted locations can be false-positive (i.e., about sixty percent of predicted locations are false-alarmed); (3) a *mle* of 0.133 indicates that damage can be located within about a distance of 0.13L (13 percent of span length) from the correct location of damage; and (4) a *mse* of 0.75 indicates that the estimated severities show an average 75 percent error and it consistently overestimates severity levels by about 1.75 times of the true damage sizes.

Secondly, for Damage Index B, the accuracy measures are interpreted as follows: (1) all localization error measures (*dme*, *fae*, and *mle*) are zero (i.e., there are no localization errors) and (2) a *mse* of 0.853 indicates that the estimated severities show an average 85.3 percent error and it consistently underestimates severity levels by about 0.15 times of the true damage sizes. Finally, for Damage Index C, the accuracy measures are interpreted as follows: (1) all localization error measures are zero (i.e., there are no localization errors) and (2) a *mse* of 0.077 indicates that the estimated severities show an average 7.7 percent error. As listed in Table 2, the predicted severities are very close to the true damage sizes. Compared to two other NDD algorithm, Damage Index C enhanced the accuracy of the damage localization and severity estimation results. (The relative impact of the uncertainty related to modeling errors or measurement errors will be examined as an extended study, although existing algorithms show their robustness in the uncertainty circumstances (See Ref. 16).)

Table 3 Quantification of damage prediction accuracy

Damage Detection Algorithm Type	Simulated Damage Predicted Damage			
	dme	*fae*	*mle*	*mse*
Damage Index A	0.083	0.570	0.133	0.570
Damage Index B	0	0	0	0.853
Damage Index C	0	0	0	0.077

5. Summary and Conclusions

The objective of this paper was to present an improved vibration-based damage detection algorithm which was newly-derived and to evaluate the accuracy of the algorithm when applied to a two-span continuous beam. This objective was achieved in two parts. In the first part, we reviewed existing damage detection algorithms and their limits in the accuracy of damage detection. Then we formulated a new damage detection algorithm which overcomes the limits of the existing algorithms and improved its accuracy in damage localization and severity estimation. In the second part, two existing algorithms and the new algorithm were evaluated by predicting damage location and severity estimation in a theoretical model of a two-span continuous beam. Each algorithm was assessed by quantifying the accuracy of damage localization and severity estimation results.

By applying the approach to the numerical example, we obtained the following relatationships between the algorithms and their accuracy in damage prediction. First, the use of Damage Index A for the damage prediction exercises resulted in (1) relatively small Type I error(false detection of true damage locations), (2) small localization error, (3) relatively high Type II error(prediction of locations that are not damaged), and (4) high severity estimation error. It consistently overestimated severities of damage by about 1.75 times of the true damage sizes. Second, the use of Damage Index B resulted in no error related to damage localization but high severity estimation error. It consistently underestimated severities by about 0.15 times of the true damage sizes. Finally, the use of Damage Index C resulted in no error related to damage localization and very small severity estimation error. Compared to two other algorithms, Damage Index C enhanced the accuracy of the damage localization and severity estimation results.

Acknowledgments

The authors wish to acknowledge the financial support of the Korean Science and Engineering Foundation, on the Korean-Japan Joint Research Project, made in the program years 1997-1999.

References

1. Kummer, E., Yang, J.C.S., and Dagalakis, N.G., "Detection of Fatigue Cracks in Structural Members", *2nd American Society of Civil Engineering/EMD Specialty Conference*, Atlanta, Georgia, 1981, pp. 445~460
2. Yang, J.C.S, Chen, J., and Dagalakis, N.G., "Damage Detection in Off-shore Structures by the Random Decrement Technique", *Journal of Energy Resources Technology*, ASME, Vol. 106, No. 1, 1984, pp.38~42
3. Flesch, R.G., and Kernichler, K., "Bridge Inspection by Dynamic Tests and Calculations Dynamic Investigations of Lavent Bridge", *Workshop on Structural Safety Evaluation Based on System Identification Approaches*, eds. H.G. Natke and J.T.P. Yao, Vieweg & Sons, Lambrecht/Pfalz, Gernamy, 1988, pp. 433~459
4. Masri, S.F., Miller, R.K., Saud, A.F., and Caughey, T.K., "Identification of Nonlinear Vibrating Structures: Part I - Formulation", *J. of Applied Mechanics*, Vol. 54, 1987, pp.923~929
5. Natke, H.G., and Yao, J.T.P., "System Identification Methods for Fault Detection and Diagnosis", *Int. Conf. on Structural Safety and Reliability*, ASCE, New York, 1990, pp.1387~1393

6. Gudmunson, P., "Eigenfrequency Changes of Structures Due to Cracks, Notches or Other Geometrical Changes", *J. Mech. Phys. Solids*, Vol. 30, No. 5, 1982, pp.339~353
7. Gudmunson, P., "The Dynamic Behavior of Slender Structures with Cross-Sectional Cracks", *J. Mech. Phys. Solids*, Vol. 31, No. 4, 1983, pp.329~345
8. Cristides, S., and Barrs, A.D.S., "One-Dimensional Theory of Cracked Bernoulli-Euler Beams", *Int. J. Mech. Science*, Vol. 26, No. 11/12, 1984, pp.639~648
9. Adams, R.D., Cawley, P., Pye, C.J., and Stone, B.J., "A Vibration Techniques for Non-Destructively Assessing the Integrity of Structures", *J. Mech. Engr. Science*, Vol.20, 1978, pp.93~100
10. Cawley, P., and Adams, R.D., "The Location of Defects in Structures from Measurements of Natural Frequencies", *J. Strain Analysis*, Vol. 14, No. 2, 1979, pp.49~57
11. O'Brien, T.K., "Stiffness Change As A Nondestructive Damage Measurement", *Mechanics of Non-destructive Testing*, ed. W.W. Stinchcomb,Plenum Press, 1980, pp.101~121
12. Kenley, R.M., and Dodds, C.J., "West Sole WE Platform: Detection of Damage by Structural Response Measurements", *Offshore Tech. Conf.*, Houston, Texas, 1980, pp.111~118
13. Biswas, M., Pandey, A.K., and Samman, M.M., "Modal Technology for Damage Detection of Bridges", *NATO Advanced Research Workshop on Bridge Evaluation, Repair and Rehabilitation*, ed. A. Nowak, Kluwer Academic Publishers, Maryland, 1990, pp.161~174
14. Stubbs, N., and Osegueda, R., "Global Non-Destructive Damage Evaluation in Solids", *Int. J. Anal. Exp. Modal Analysis*, Vol. 5, No. 2, 1990, pp.67~79
15. Chen, J., and Garba, J.A., "On-Orbit Damage Assessment for Large Space Structures", *AIAA Journal*, Vol. 26, No. 9, 1988, pp.1119~1126
16. Kim, J.T., and Stubbs, N., "Model-Uncertainty Impact and Damage-Detection Accuracy in Plate Girder", *J. of Structural Engineering*, ASCE, Vol. 121, No. 10, 1995, pp.1409~1417
17. Stubbs, N., and Kim, J.T., "Damage Localization in Structures Without Baseline odal Parameters", *AIAA Journal*, AIAA, Vol. 34, Bo. 8, 1996, pp.1644~1649
18. Aktan, A.E., Lee, K.L., Chuntavan, C., and Aksel, T., "Model Testing for Structural Identification and Condition Assessment of Constructed Facilities", *Proc. 12th Int. Modal Analysis Conference*, Vol. 1, 1994, pp.462~468
19. Fukunaga, K., *Introduction to Statistical Pattern Recognition*, Academic Press, New York, 1990
20. Gibson, J.D., and Melsa, J.L., *Introduction to Nonparametric Detection with Applications*, Academic Press, New York, 1975
21. Kosko, B., *Neural Networks for Signal Processing*, Prentice Hall, New Jersey, 1992

(접수일자 : 1999. 2. 9)